Dig Dis Sci (2011) 56:731–740
DOI 10.1007/s10620-010-1347-6

ORIGINAL ARTICLE

Analysis of Biliary Epithelial-Mesenchymal Transition in Portal Tract Fibrogenesis in Biliary Atresia

Yu-Hua Deng · Cong-Lun Pu · Ying-Cun Li · Jin Zhu · Chunping Xiang · Ming-Man Zhang · Chun-Bao Guo

Received: 23 February 2010 / Accepted: 12 July 2010 / Published online: 20 August 2010

Abstract
Background The cellular origin of myofibroblast in the liver fibrosis remains unclear. This study was designed to investigate whether biliary epithelial cells (BECs) undergoing epithelial–mesenchymal transition (EMT) might be found in patients with biliary atresia, thereby serving as a source of fibrotic myofibroblasts.
Methods Liver sections from patients with biliary atresia were evaluated to detect antigen for the BECs marker 4 and cytokeratin-7 (CK-7), proteins (fibroblast-specific protein 1, also known S100A4; the collagen chaperone heat shock protein 47, HSP47) characteristically expressed by cells undergoing EMT, as well as myofibroblasts marker a-smooth muscle actin (a-SMA).
Results Normal bile ducts BECs could express CK-7 and low levels of a-SMA; they did not express S100A4 and HSP47. However, BECs from biliary atresia resulted in increased expression of a-SMA, S100A4, with concurrent transition to a fibroblast-like morphology and decreased expression of AK-7. Furthermore, BECs in biliary atresia were associated with significant bile ductular proliferation and coexpressed both epithelial and mesenchymal markers.
Conclusions From significant histologic evidence, the BECs forming small- and medium-sized bile ducts undergoing EMT may account for prominent bile ductular proliferation and directly contribute to fibrogenesis in BA.

Keywords Epithelial-mesenchymal transition · Biliary atresia · Fibrogenesis · S100A4

Abbreviations

EMT	Epithelial–mesenchymal transition
aSMA	a-Smooth muscle actin
BECs	Biliary epithelial cells
CK-7	Cytokeratin-7

Introduction

Biliary atresia is the most common progressive liver disease of infancy, causing atresia of the major extrahepatic and intrahepatic biliary ducts that lead to cirrhosis [1]. Damage to the small- and medium-sized intrahepatic bile ducts is a characteristic feature of biliary atresia and generally evokes a compensatory repair response that involves expansion of portal tracts with proliferating bile ductules even at end-stage [2]. With time, the fibroproliferative response bridge adjacent portal areas and culminate in biliary cirrhosis. Thus, chronic cholestatic liver damage results, at least in part, from unsuccessful repair of biliary injury [3].

During chronic fibrogenesis, the matrix deposition from myofibroblasts are thought capable of matrix synthesis. Epithelial–mesenchymal transition (EMT) is a well-recognized mechanism for forming myofibroblasts in

The authors Yu-Hua Deng and Cong-Lun Pu contributed equally to this work.

Y.-H. Deng · C.-L. Pu · Y.-C. Li · M.-M. Zhang · C.-B. Guo (✉)
Department of Hepatobiliary Surgery, Children's Hospital of Chongqing Medical University, 136 Zhongshan 2nd Rd., Chongqing 400014, People's Republic of China
e-mail: gchunbao@yahoo.com.cn

J. Zhu · C. Xiang
Department of Pathology, Children's Hospital, Chongqing Medical University, Chongqing 400014, People's Republic of China

injured tissues [4, 5]. It is a process in which mature epithelial cells lose the appearance, cell–cell contacts, and unique protein expression patterns of epithelia such as E-cadherin and 4 and cytokeratin-7 (CK-7), and at the same time acquire the phenotypic characteristics of mesenchymal cells and fibroblast markers including S100A4 (the human homologue of fibroblast-specific protein-1 [FSP-1]), vimentin, matrix metalloproteinases (MMP) 2 and 9, and a-smooth muscle actin (aSMA) [6]. Immunostaining of serial liver sections from patients with primary biliary cirrhosis (PBC) demonstrated expression of vimentin and other mesenchymal markers in proliferating biliary epithelial cells (BECs) within fibrotic portal tracts [7, 8]. This lead the authors to propose that EMT may also play a role in the pathogenesis of biliary fibrosis during biliary atresia. Because the development of hepatic fibrosis in biliary atresia is more rapid and aggressive than any other disorder in adults and there is pronounced early bile ductular proliferation in this disease, we hypothesized that BECs in biliary atresia undergoing EMT would potentially explain the rapidity of the portal fibrosis and biliary cirrhosis. Demonstration of the contribution of EMT to hepatic fibrosis observed in biliary atresia may suggest a new basis for understanding their pathogenesis and potential novel treatment to promote normal re-epithelialization of the injured biliary tree.

This study was designed to determine whether BECs in biliary atresia undergoing EMT are the cellular source of increased collagen production in infants with biliary atresia by analyzing liver samples from surgery. Sections from patients with biliary atresia and a variety of other chronic cholestatic diseases were then examined by immunohistochemistry to provide evidence for significant EMT in biliary atresia.

Materials and Methods

Liver Tissue Collection and Patient Characteristics

Liver biopsies were obtained from chronic cholestatic patients who were referred to the affiliated hospital of Chongqing Medical University, Chongqing, P. R. China, with detailed clinical data. All subjects were ethnic Chinese. This study was performed according to a protocol approved by the Institutional Review Board of the Chongqing Medical University, Chongqing, People's Republic of China in accordance with the ethical standards prescribed by the Helsinki Declaration of the World Medical Association. Written informed consent was obtained from the parents prior to specimen collection.

The study consisted of 16 patients with pathologically confirmed biliary atresia (perinatal form) during Kasai portoenterostomy. Patients were excluded if they had any virus infection, including hepatitis B surface antigen positive, the human immunodeficiency virus, were CMV positive, or had renal failure or hepatocellular carcinoma. Additionally, these patients would be excluded if they were receiving experimental treatment trial or were unable to have regular hepatic function assessments. Control liver tissues were obtained from cholestatic disease patients with comparable age to the BA patients (cholestatic controls), including infants who had severe cholestasis requiring intraoperative cholangiogram to rule out biliary atresia (neonatal hepatitis, $n = 5$). Cholestatic disease was chosen because of clinical and histologic similarities. Non-cholestatic (normal) controls included five percutaneous liver biopsy under general anesthetic. All diagnoses were based on clinical and laboratory data and on histopathological examination of histological samples.

Among the 16 patients, extrahepatic bile duct remnant tissues and wedge liver biopsies were obtained from BA patients at the time of the Kasai procedure, termed as hepatoportoenterostomy biopsies. All the patients were referred for living-related liver transplantation assessment because of progressive liver disease; the liver biopsies were obtained from the excised livers, termed as post-hepatoportoenterostomy biopsies. Normal pediatric samples were obtained from autopsies in cases where the cause of death was unrelated to the liver. At the time of the liver biopsy, all the surgical samples were divided into two portions. A portion was placed in 10% neutral buffered formalin, fixed overnight, and embedded in paraffin for routine histological examination and immunohistochemistry. Part of samples were simultaneously placed in OCT freezing media or wrapped in aluminum foil, snap-frozen in liquid nitrogen, and stored at −70°C until analysis. Portal, periportal and lobular fibrosis were determined in a blinded fashion on all liver biopsies by an experienced liver pathologist.

Immunohistochemistry

For immunohistochemical cellular colocalization of epithelial and mesenchymal markers, formalin-fixed, paraffin-embedded liver tissue samples were obtained and sliced. Contiguous 3-μm formalin-fixed, paraffin-embedded sections were first submitted to rehydrate by incubating successively in 100, 90, and 70% ethanol. Heat-induced epitope retrieval was performed in 10 mM citric acid (pH 6.0) in a 1,200-Watt microwave oven at 90% output. Endogenous peroxidases were blocked with 2% hydrogen peroxide followed by avidin/biotin blocking (Vector Laboratories, Inc, Burlingame, CA) and nonspecific antibody binding (Protein Blocking Agent, Coulter-Immunotech, Fullerton, CA). For single labeling, antibody incubations and detection

were carried out with the primary antibody at appropriate dilutions overnight at 4°C. Immunohistochemistry was performed using the following antibodies: S100A4 (1:80 dilution, mouse clone, Santa Cruz Biotechnology Inc., Santa Cruz, CA) and CK-7 (1:40 dilution, mouse clone, Santa Cruz Biotechnology Inc., Santa Cruz, CA). Next, the tissue sections were incubated with a 1:300 dilution of biotinylated secondary antibodies (goat antimouse immunoglobulins, Shanghai Sangon Biotech, Shanghai, China) for 30 min. After development of the color with diaminobenzidine, the slides were counterstained with hematoxylin. Appropriate positive and negative control slides were run in parallel with study slides, which included an isotype-matched immunoglobulin at the same concentration as that of the primary antibody. Slides were dehydrated through serial ethanol washes, cleared in xylene, and mounted. Slides were visualized using a Nikon E600 microscope (Nikon, Melville, NY) at ×400, and images were captured with a cooled charge-coupled device camera (Magnafire; Olympus) equipped with a MicroColor liquid crystal for color imaging. Captured images were imported into Adobe Photoshop (Adobe Systems) as TIFF files. For quantification, 20 high-power fields were examined for each tissue slide for each patient ($n = 3$). Cells with cytosol/membranes that strongly stained for CK-7 or S100A4 were considered to be positive. All slides were independently analyzed by two blinded researchers.

Double-Label Immunofluorescence

To study coexpression of different markers in the different reactive cellular elements, dual immunofluorescence staining was performed on cryosections (4 μm) by using different combinations of antibodies. Samples were fixed and permeabilized, saturated, and processed for immunostaining with primary fluorescein isothiocyanate (FITC)-labled antibody S100A4 and cytokeratin-7 (CK-7; Santa Cruz Biotechnology Inc., Santa Cruz, CA). Following 1-h incubation at room temperature with FITC-conjugated antibody, tissue sections were rinsed and then incubated with the secondary antibody (dilution, 1:20; incubation, 30 min; DAKO). Antigen retrieval was then performed by heating the filters in an antigen-unmasking solution (Vector), cooling slowly, and rinsing. Tissue sections were then incubated for 45 min with the second primary antibody, including vimentin (dilution, 1:40), aSMA (dilution, 1:40), and HSP47 (dilution, 1:80) antibody (Santa Cruz Biotechnology Inc., Santa Cruz, CA). After extensive washing, the slides were incubated with the secondary antibody Texas Red-conjugated horse anti-mouse (dilution, 1:20; incubation, 30 min; Vector Laboratories, Burlingame, CA). Counterstaining with 4_,6-diamidino-2-phenylindole (DAPI) was employed to demonstrate nuclei.

To decrease background fluorescence in formalin-fixed tissue, the sections were incubated in 0.3% Sudan Black for 10 min at room temperature followed by four washes in TBS before mounting. Filters were then rinsed, mounted on slides using Vectashield mounting medium (without propidium iodide), and coverslipped. In control experiments, the order of primary antibodies was switched to confirm the specificity of labeling (not shown). As a negative control, the primary antibody was replaced with nonimmune IgG for the second staining step, and no staining confirmed the specificity of the secondary antibody. In addition, sequential sections of some samples were single stained to confirm double-staining data.

Immunofluorescence-labelled preparation sample images were analysed using the Leica DMRA2 microscope (Leica Microsystems Inc., Bannockburn, IL). For two-colour labelled specimens, the fluorochromes were sequentially imaged to avoid possible 'crosstalk' between the two emission spectra. The areas of interest were selected and spectral unmixing was accomplished by using Nuance software v1.42 (Cambridge Research and Instrumentation, Inc.) with pure spectral libraries of individual chromogens. Images were collected using a digital camera (Nikon) and analyzed by Photoshop 5.0 software (Adobe, San Jose, CA). For quantification, the total number of cells positive for epithelial marker (S100A4) was counted by dividing the number by a specific second marker in each field.

Results

Histopathological Assessment of Biliary Atresia Pre- and Post-Kasai Hepatoportoenterostomy

The patients with biliary atresia, cholestatic controls and normal controls were analyzed and had conjugated hyperbilirubinemia and elevated serum GGTP levels. Table 1 presents demographic data and serum bilirubin and GGTP values from each patient group. Because the extrahepatic bile duct is the primary target in biliary atresia, extrahepatic bile duct remnant tissues as well as liver tissue were investigated.

The presence of periportal and bridging fibrosis was documented by H&E and Hematoxylin/van Gieson staining of a portion of each tissue specimen collected, as shown in Fig. 1. Among them, 16 patients were examined both pre- and post-Kasai procedure. Histology of cholestasis from biliary atresia and liver disease other than BA revealed enlarged bile duct surrounded by excessive collagen protein deposition and bile plugs. Extensive periductal canalicular and cellular biliary stasis and bile duct hyperplasia with expanded portal tracts was observed within the portal tracts and extrahepatic bile duct remnants (data not shown)

Table 1 Summary of perioperative characteristics based on recipient previous Kasai operation

Characteristics	Biliary atresia ($N = 13$)	Choledochal cysts ($N = 3$)	Neonatal hepatitis ($N = 5$)	Normal ($N = 5$)
Age (month)	2.89 ± 3.12	10.27 ± 4.32	3.89 ± 3.12	8.89 ± 11.67
Weight (kg)	5.4 ± 1.4	7.4 ± 2.6	7.2 ± 3.8	6.6 ± 1.9
TB (2.0–20), umol/L	216 ± 103	68 ± 34	126 ± 58	8.9 ± 2.1
DB (0–4), umol/L	169 ± 82	33 ± 21	78 ± 45	2.5 ± 1.2
γGT (0–50), U/L	269 ± 166	162 ± 76	154 ± 87	36 ± 24
Albumin (33–52), g/L	31 ± 9	37 ± 9	36 ± 11	41 ± 8

TB total bilirubin, *DB* direct bilirubin, *γGT* gumma glutamyl transferase

Values are given as mean ± standard deviation

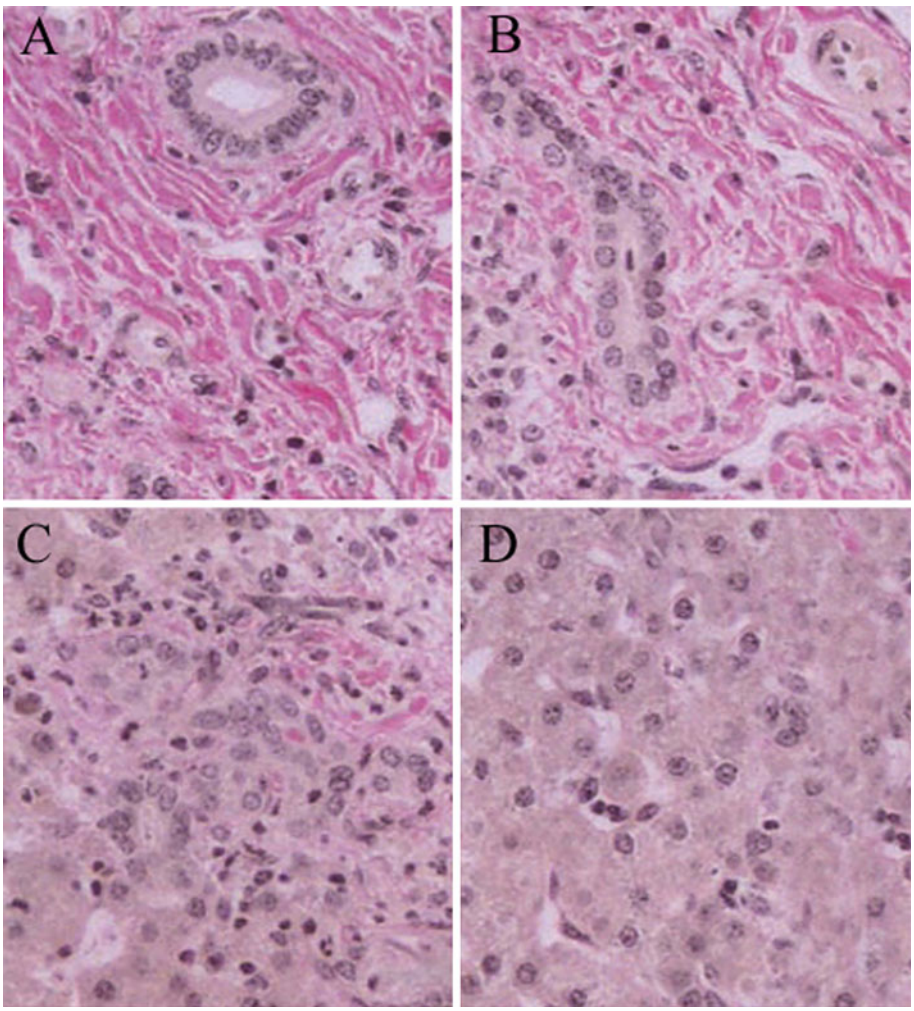

Fig. 1 Representative hematoxylin and eosin stain of liver from BA and control tissue. Hematoxylin/van Gieson stain at the time of Kasai procedure (**a**) and transplant (**b**) demonstrating a portal tract with bile duct proliferation and fibrosis (*pink*) extending into the parenchyma. The degree of fibrosis is similar in samples taken at the time of Kasai operation and transplant in which matched specimens were examined. Serial section from control subjects (**c**, neonatal hepatitis) and normal control (**d**) stained with hematoxylin/van Gieson demonstrating mild portal tract fibrosis and no significant fibrosis, respectively. Original magnifications: ×240 (**a**–**d**). (Color figure online)

of BA patients. Fibroblastic cells were seen particularly in the extracellular matrix surrounding both portal tracts and hyperplastic bile ducts, and within fibrous septa bridging between portal tracts.

Mild to severe portal tract cirrhosis in all biopsies was examined, including pre- and post-Kasai hepatoportoenterostomy livers. Eight patients had fibrosis of moderate severity and five patients had severe fibrosis. The severity of limiting plate disruption was variable and was not associated with the severity of established fibrosis. Only one patient showed a decrease in the severity of fibrosis and hence in the number of hyperplastic bile ducts and within fibrous bridging septa after Kasai hepatoportoenterostomy. The remainder of cholestatic controls revealed the usual spectrum of cholestasis, bile duct proliferation, steatosis, and portal fibrosis (Fig. 1). Five biopsies from

control tissue revealed no significant fibrosis, of which five revealed steatosis only.

Evidence of EMT During Liver Fibrosis

It has been implicated that certain epithelial cells in injured livers undergo epithelial-to-mesenchymal transition (EMT) and move into the hepatic mesenchyme where they exhibit fibroblastic features [9]. To test for the role of EMT in the formation of fibrosis in BA tissue, we examined liver and sections for expression of S100A4, a marker of fibroblastic transformation of epithelial cells. Bile duct epithelium were identified by characteristic vessel formation and confirmed by cytokeratin 7 staining (Fig. 2a). The livers of cholestatic patients showed clear expression of S100A4 within BECs of small and medium-sized bile ducts, as well as adjacent stroma (Fig. 2b). The small bile ducts instead of medium-sized bile ducts in sections with cholestatic controls expressed low levels of S100A4 (Fig. 2c) indicating a response to non-specific damage. Matched serial sections in controls showed no expression associated with the epithelial cells (Fig. 2d), except for occasional immune cells.

To verify that this mesenchymal marker was truly expressed by epithelial cells, the intermediate phenotype were investigated to observe double immunostaining for S100A4 and CK-7, which define a potentially motile

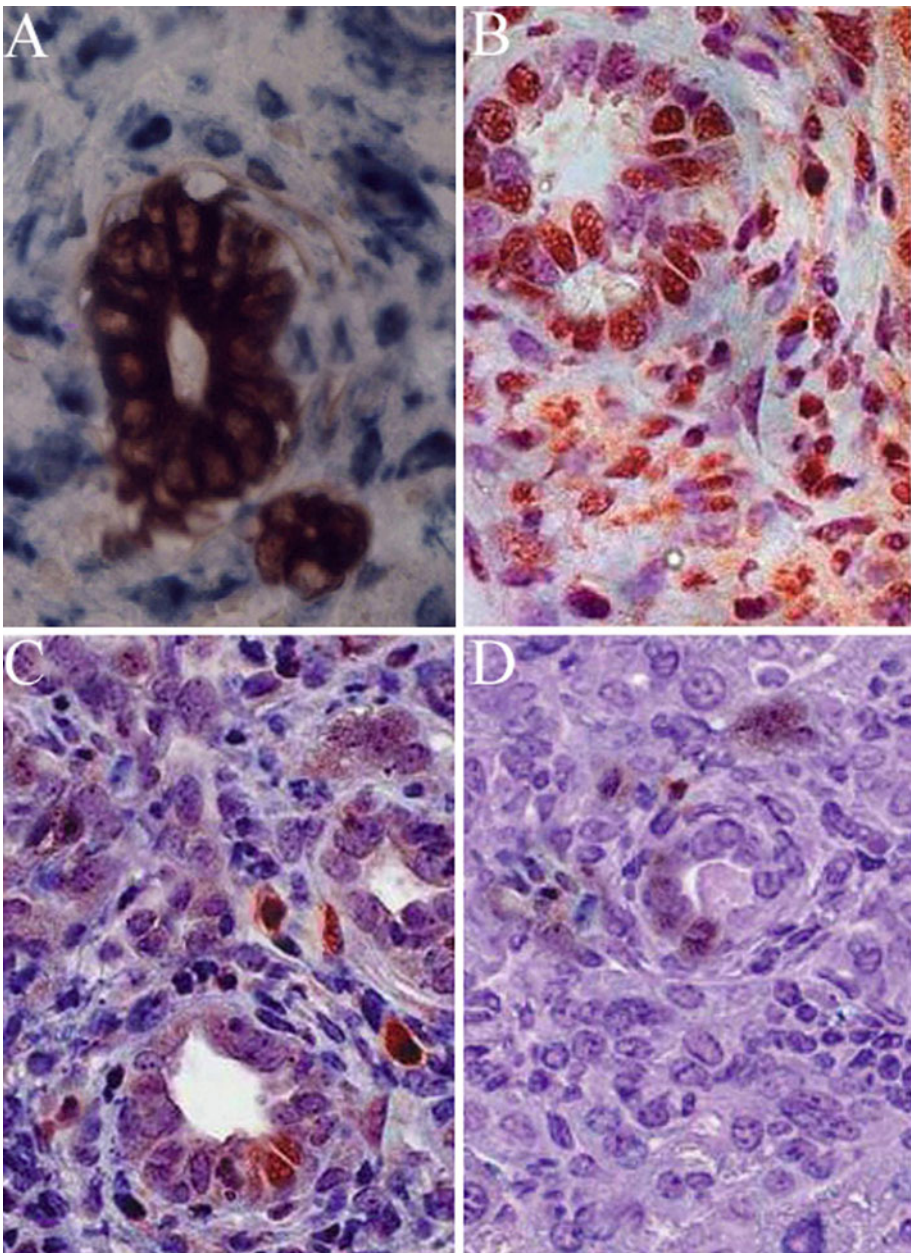

Fig. 2 A representative series of immunohistochemical results from liver tissues of patients with BA, neonatal hepatitis, and normal controls showing expression of CK-7 and S100A4. Immunohistochemistry for CK-7 expression (expected *deeply-brown*) in liver sections from a child with BA demonstrating expression of CK-7 in BECs forming a small intrahepatic bile duct, hyperplastic bile ductules in expanded portal tracts and at the growing margin of the scar tissue formation (**a**). S100A4 immunohistochemistry of liver sections demonstrated an S100A4-expressing epithelial cell (*brown*) within a ductule together with S100A4 expression within fibroblast-like cells localized in the interstitial compartment (**b**) from BA and nonspecific faint brown cytoplasmic staining from neonatal hepatitis (**c**) and normal liver tissues (**d**). Original magnification ×360 for **a**, ×360 for (**b**–**d**). (Color figure online)

population of cells with an epithelial phenotype undergoing localised EMT during chronic cholestatic liver disease in humans. Sections of normal human liver showed clear, localised expression of CK-7, defining the epithelial cells lining the intrahepatic bile ducts (Fig. 3). There were no merged signals among ductular cells or the surrounding tissues to suggest EMT activity in the normal liver at the time of tissue acquisition. Coexpression of S100A4 and CK-7 (Fig. 3) was confirmed in bile ducts and in the ductular reaction within the cholestatic tissue (about 30–50% of CK-7-positive ductular cells) and revealed a mixture of epithelial and interstitial cell reaction products amidst this injured tissue. Gain of S100A4 expression also coincided with decreased staining for the epithelial marker CK-7 (Fig. 3). There was evidence of biliary epithelium undergoing disaggregation in an obstructed biliary duct stained yellow on merged color under confocal microscopy (white arrow). Some of these S100A4-expressing

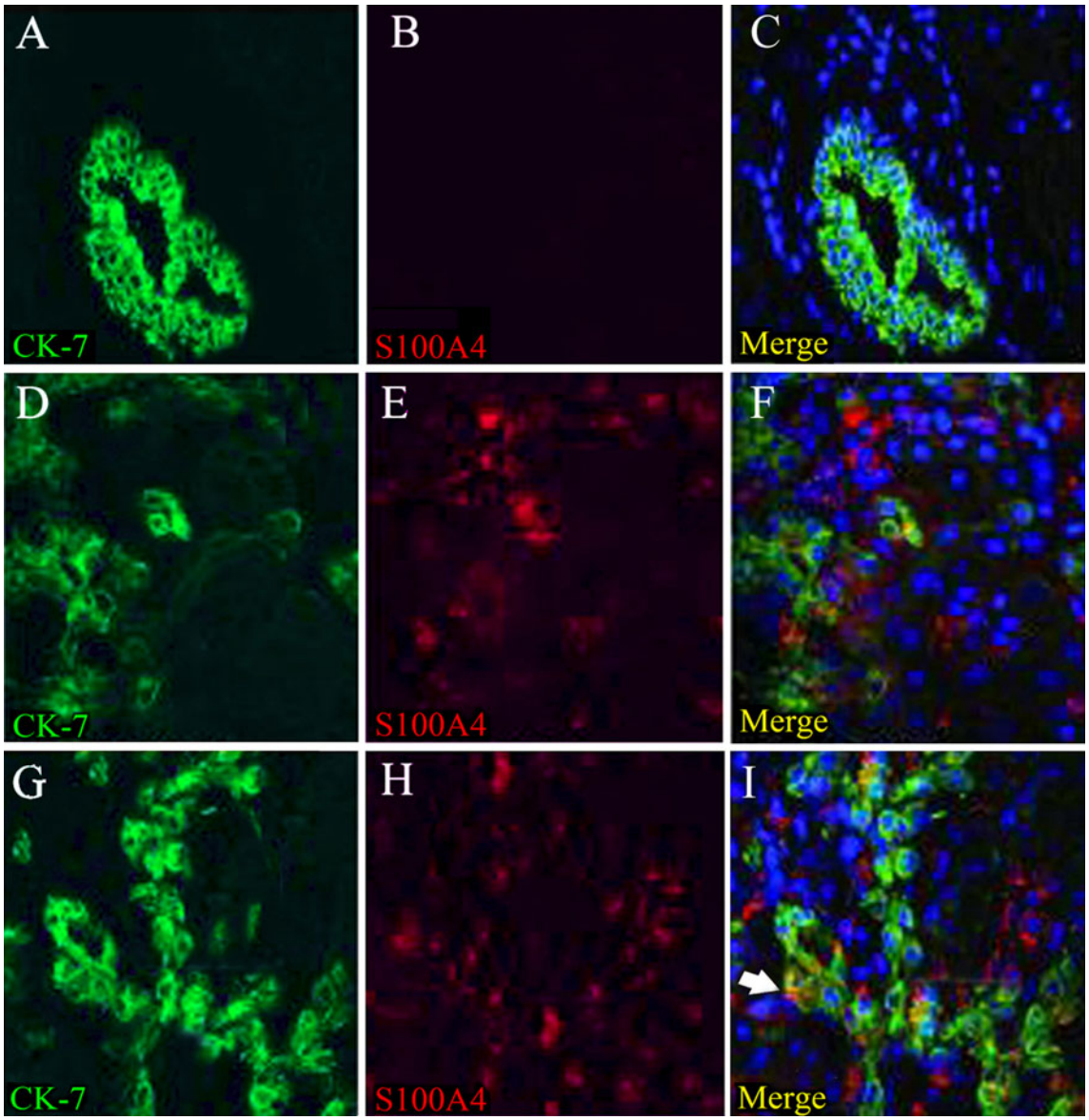

Fig. 3 Double immunofluorescence staining showed the localization of CK-7 (*green*, *left column*) and S100A4 (*red*, *center column*) in the liver sections from liver tissues of patients with BA, neonatal hepatitis and normal controls. Merging of CK-7 and S100A4 staining is presented *yellow* in the *right column*. Colocalization of CK-7 and S100A4 is clearly evident in the bile duct epithelium of BA patients. The *arrow* denotes a cluster of cells that retained bile duct epithelial cell appearance, but lost CK-7, and were S100A4-positive. Patient samples included normal control from percutaneous liver biopsy **a–c**; neonatal hepatitis, samples intraoperative cholangiogram **d–f**; and biliary atresia, samples from Kasai operation **g–i**. All photos were taken at original magnification ×240. (Color figure online)

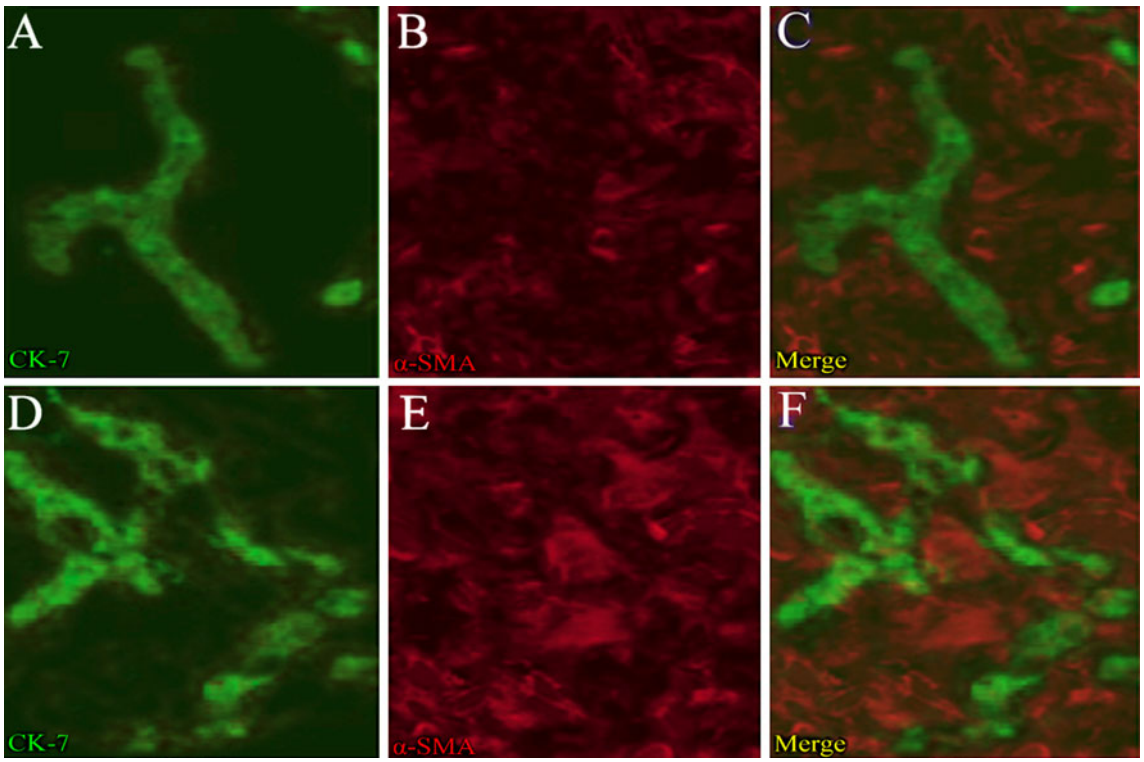

Fig. 4 Colocalization of the bile duct epithelial marker CK-7 (*green*, *left column*) and myofibroblast marker a-SMA (*red*, *center column*) were indicated in the *right column*. A small bile duct confirms no coexpression of CK-7 and aSMA with samples from both BA (**a**–**c**) and neonatal hepatitis (**d**–**f**). Original magnification ×360. (Color figure online)

transitional epithelial cells also began to take the shape of fibroblasts, which could penetrate the matrix and migrate out of the ductular structure.

We also co-stained biliary atresia livers with CK-7 and α-SMA, but did not observe marker colocalization, although multiple α-SMA-positive cells lay at the growing margin of the scar tissue formation, where the stellate-shaped morphology of myofibroblasts were clearly present (Fig. 4). This suggests that cells at this stage will have lost epithelial markers.

Demonstration of EMT-Derived Fibroblasts in Fibrotic Liver Tissue

In order to identify the cellular source of increased collagen leading to hepatic fibrosis in BA, liver biopsies were further examined histologically to identify the contribution of bile duct epithelium-derived fibroblasts to the overall activated fibroblast population. Figure 5a demonstrates increased numbers of morphological fibroblastic cells surrounding the same enlarged bile duct, showing co-localization of

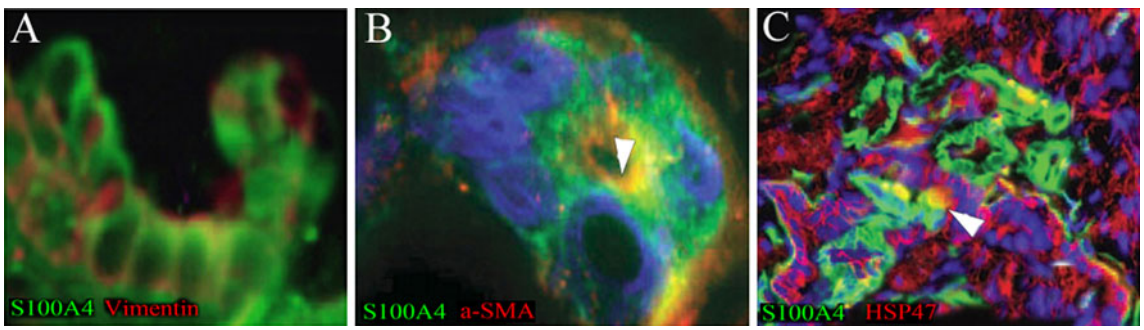

Fig. 5 Evidence for EMT in BA with bile duct proliferation. Liver tissue was examined for evidence of EMT by coexpression (*yellow*) of S100A4 (*green*) with vimentin, aSMA, and HSP47 (*red*), respectively. Colocalization is seen in BECs in BA in which there is bile duct proliferation (*yellow*). **a** Coexpression (*yellow*) of S100A4 (*green*) and vimentin. **b** Coexpression (*yellow*) of S100A4 (*green*) and aSMA (*red*). **c** Coexpression (*yellow*) of S100A4 (*green*) and HSP47 (*red*). Magnification, ×200 for **a**, ×360 for **b**, ×100 for **d**. (Color figure online)

S100A4 (green) and vimentin (red), the early marker for the development of hepatic fibrosis in these patients, in the identical region of increased collagen protein deposition. The bile ducts in sections from normal controls were negative for both S100A4 and vimentin (data not shown).

Because it is difficult to directly determine which cells in a fibrotic reaction contribute to interstitial collagen production by measuring intracellular collagen synthesis in vivo, we used the surrogate marker HSP47, recognizing Xaa-Arg-Gly motifs in the collagen triple helix, which abundantly increases to chaperon type I collagen molecules in cells actively engaged in ongoing collagen synthesis. Double staining for S100A4 (green) and HSP47 (red; Fig. 5b) in the biliary tree in a significant number developed yellow on merged color, indicating that these populations of cells during EMT contribute collagen to the fibrogenic response. So it is implicated that epithelial cells in bile ducts and ductules associated with the EMT are the cellular source of increased collagen leading to hepatic fibrosis in hepatic fibrosis of BA. Normal bile ducts did not coexpress both S100A4 and vimentin or HSP47 (data not shown).

Myofibroblasts, the terminal cells in EMT in fibrosis, which could express aSMA, were observed in areas of established fibrosis (Fig. 5c) ranging in distribution from mild-periportal to pan-lobular. Normal bile ducts did not express aSMA co-stained with S100A4, and the myofibroblast marker protein α-SMA in biliary atresia livers was seen in extrahepatic as well as intrahepatic ducts from BA patients (Fig. 5c).

Discussion

This study has provided strong evidence for EMT in biliary atresia related liver fibrosis in response to epithelial cell injury. Our data demonstrated BECs could serve as a source of myofibroblasts to contribute significantly to portal tract fibrosis in biliary atresia. BECs in biliary atresia, identified by the localization of CK-7, are responsible for the production of increased levels of type I collagen leading to hepatic fibrosis. Importantly, the stimulated BECs adopted a fibroblastic morphology with increased cytoplasmic expression of the EMT marker, S100A4, which is the most consistent indication of EMT in liver fibrosis [10, 11]. We also acquired high levels of organised aSMA within the cytoplasm, which had a significantly enhanced potential to invade a basement membrane-like matrix. We also observed expression of these EMT markers in other pediatric cholestasis liver diseases characterized by bile duct proliferation, suggesting that EMT is a general response to ductular proliferation.

The relative individual contribution of bile duct epithelium-derived fibroblasts to the overall activated fibroblast population might be crucial for the progression of liver fibrosis [12]. In our study we demonstrated that the bile duct epithelium, transdifferentiation to mature myofibroblasts, may be an additional and significant lineage of fibroblasts. Determining the different myofibroblast population in biliary atresia will require morphological and ultrastructural analysis, together with validation expression of panels of characteristic immunocytochemical and biochemical markers to discern their derivation [13, 14]. Among available phenotypic markers, α-SMA remains the most reliable marker of myofibroblastic cells. The source of α-SMA in biliary atresia as evidenced by immunohistochemistry and its synthesis is generally detectable in selected subpopulations of fibroblasts located around the portal area [15, 16]. Sicklick et al. [17], studying a single human patient with biliary atresia, noted α-SMA reactivity in structures that appeared to be bile ducts. This strongly suggests epithelial cells may serve as a source of myofibroblasts in the epithelial cell/fibroblast paradigm of biliary atresia. We have also shown that hyperplastic bile duct cells acquired high levels of organised aSMA within their cytoplasm with increased cytoplasmic expression of S100A4. S100A4 directly increases cell motility through modification of actin function, so the bile duct epithelial cells also had a significantly enhanced potential to invade a basement membrane-like matrix, and at the same time lose their morphogenic cues and "select" new fates.

Because EMT is associated with a loss of epithelial markers and gain of mesenchymal markers [18], we demonstrated individual epithelial cells clearly in a transitional state by acquiring some mesenchymal antigens and losing epithelial markers in EMT. It has already been reported that primary mesenchymal cells do not express S100A4, whereas S100A4 expression is found in the epithelial phenotype within the ductular reaction resting and activated tissue fibroblasts [19–21]. We demonstrated expression of S100A4 within BECs taken from patients with biliary atresia (even at the time of Kasai operation). Reduced expression of cytokeratins was noted in bile duct epithelium undergoing EMT.

Although we observed colocalization of CK-7 and several mesenchymal markers, we did not observe colocalization of CK-7 and α-SMA in the livers of patients with biliary atresia. Demonstration of increased S100A4 expression together with low levels of CK-7 in some cells with a fibroblastic morphology also suggests the presence of some cells at an early stage after the induction of EMT. Furthermore, α-SMA is not expressed in all S100A4 positive fibroblasts. We hypothesize that coexpression of CK-7 and S100A4 presented within small bile ducts and the expression of S100A4 and vimentin precedes expression of

HSP47, whereas α-SMA appears later, after epithelial cell markers have been lost [22]. The absence of aSMA within the ductular epithelium might simply reflect the fact that cells undergoing EMT have migrated from this tissue before acquiring aSMA expression. The marker expression profiles in EMT of liver fibroblastic cells change significantly, further confounding assessment of cell lineage in our human sample. Animal models will also be required to determine the lineage-tracing spatio-temporal expression of specific markers in biliary fibrosis. Importantly, the stimulated BECs adopted a fibroblastic morphology and acquisition of a spindle shape, long cytoplasmic extensions and acquire migratory and ductular basement membrane disruption capabilities with CK7-positive cells [23], which is entirely consistent with the observed induction of MMP-2 expression in vivo [9]. This indicates that cells undergoing EMT have migrated and acquired an immature epithelial cell/fibroblast phenotype, suggesting that this phenotypic shift may explain the "loss" of BECs and "gain" of portal tract fibroblasts and eventually differentiate into aSMA-expressing myofibroblasts, which characterizes a ductopenic disease such as BA.

In this research, the presence of transitional cell coexpression of epithelial, mesenchymal markers in subpopulations of fibroblasts located around the portal area suggests that BECs undergoing EMT may serve as a source of myofibroblasts surrounding bile ductules leading to periductular fibrosis, especially in the setting of chronic liver injury, biliary atresis EMT seems to be a late response, requiring a sustained, chronic injury. EMT and other epithelial cell responses to cholestasis injury may be the true key why biliary atresia is often such a relentlessly progressive disease. In this context, the association of increased numbers of fibroblastic foci and a worse prognosis may be due to acceleration in the degree of epithelial cell injury at the time of biopsy. Such a scenario might explain the reversibility of vanishing bile duct syndrome in some situations such as post Kasai procedure.

Acknowledgments The research was supported by National Natural Science Foundation of China (No. 30973440), National Natural Science Foundation of China (No. 30770950) and key project of Chongqing Natural Science Foundation (CSTC, 2008BA0021). This work was supported by key projects of natural science foundation of China (No. 30330590). The authors wish to express their gratitude to Dr. Kaiyong Tang for providing technical assistance and insightful discussions during the preparation of the manuscript, without whom this work would not have been possible. We thank Dr Xiaoyong Zhang, at the Wistar Institute, USA, for help with the linguistic revision of the manuscript.

References

1. Narayanaswamy B, Gonde C, Tredger JM, Hussain M, Vergani D, Davenport M. Serial circulating markers of inflammation in biliary atresia—evolution of the post-operative inflammatory process. *Hepatology*. 2007;46(1):180–187.
2. Fabris L, Cadamuro M, Guido M, et al. Analysis of liver repair mechanisms in Alagille syndrome and biliary atresia reveals a role for notch signaling. *Am J Pathol*. 2007;171(2):641–653.
3. Ramm GA, Nair VG, Bridle KR, Shepherd RW, Crawford DH. Contribution of hepatic parenchymal and nonparenchymal cells to hepatic fibrogenesis in biliary atresia. *Am J Pathol*. 1998;153(2):527–535.
4. Zeisberg M, Yang C, Martino M, et al. Fibroblasts derive from hepatocytes in liver fibrosis via epithelial to mesenchymal transition. *J Biol Chem*. 2007;282(32):23337–23347.
5. Iwano M, Plieth D, Danoff TM, Xue C, Okada H, Neilson EG. Evidence that fibroblasts derive from epithelium during tissue fibrosis. *J Clin Invest*. 2002;110(3):341–350.
6. Choi SS, Diehl AM. Epithelial-to-mesenchymal transitions in the liver. *Hepatology*. 2009;50(6):2007–2013.
7. Díaz R, Kim JW, Hui JJ, et al. Evidence for the epithelial to mesenchymal transition in biliary atresia fibrosis. *Hum Pathol*. 2008;39(1):102–115.
8. Harada K, Sato Y, Ikeda H, et al. Epithelial-mesenchymal transition induced by biliary innate immunity contributes to the sclerosing cholangiopathy of biliary atresia. *J Pathol*. 2009;217(5):654–664.
9. Rygiel KA, Robertson H, Marshall HL, et al. Epithelial-mesenchymal transition contributes to portal tract fibrogenesis during human chronic liver disease. *Lab Invest*. 2008;88(2):112–123.
10. Kalluri R, Neilson EG. Epithelial-mesenchymal transition and its implications for fibrosis. *J Clin Invest*. 2003;112(12):1776–1784.
11. Postlethwaite AE, Shigemitsu H, Kanangat S. Cellular origins of fibroblasts: possible implications for organ fibrosis in systemic sclerosis. *Curr Opin Rheumatol*. 2004;16(6):733–738.
12. Friedman SL. Mechanisms of hepatic fibrogenesis. *Gastroenterology*. 2008;134(6):1655–1669.
13. Novo E, di Bonzo LV, Cannito S, Colombatto S, Parola M. Hepatic myofibroblasts: a heterogeneous population of multifunctional cells in liver fibrogenesis. *Int J Biochem Cell Biol*. 2009;41(11):2089–2093.
14. Choi SS, Omenetti A, Witek RP, et al. Hedgehog pathway activation and epithelial-to-mesenchymal transitions during myofibroblastic transformation of rat hepatic cells in culture and cirrhosis. *Am J Physiol Gastrointest Liver Physiol*. 2009;297(6):G1093–G1106.
15. Shteyer E, Ramm GA, Xu C, White FV, Shepherd RW. Outcome after portoenterostomy in biliary atresia: pivotal role of degree of liver fibrosis and intensity of stellate cell activation. *J Pediatr Gastroenterol Nutr*. 2006;42(1):93–99.
16. Lewindon PJ, Pereira TN, Hoskins AC, et al. The role of hepatic stellate cells and transforming growth factor-beta(1) in cystic fibrosis liver disease. *Am J Pathol*. 2002;160(5):1705–1715.
17. Sicklick JK, Choi SS, Bustamante M, et al. Evidence for epithelial-mesenchymal transitions in adult liver cells. *Am J Physiol Gastrointest Liver Physiol*. 2006;291(4):G575–G583.
18. Taura K, Miura K, Iwaisako K, Osterreicher CH, Kodama Y, Penz-Österreicher M, Brenner DA. Hepatocytes do not undergo epithelial-mesenchymal transition in liver fibrosis in mice. *Hepatology*. 2010;51(3):1027–1036.
19. Guarino M, Tosoni A, Nebuloni M. Direct contribution of epithelium to organ fibrosis: epithelial-mesenchymal transition. *Hum Pathol*. 2009;40(10):1365–1376.
20. Robertson H, Kirby JA, Yip WW, Jones DE, Burt AD. Biliary epithelial-mesenchymal transition in posttransplantation recurrence of primary biliary cirrhosis. *Hepatology*. 2007;45(4):977–981.

21. Friedman SL. Mechanisms of disease: mechanisms of hepatic fibrosis and therapeutic implications. *Nat Clin Pract Gastroenterol Hepatol*. 2004;1(2):98–105.
22. Vongwiwatana A, Tasanarong A, Rayner DC, Melk A, Halloran PF. Epithelial to mesenchymal transition during late deterioration of human kidney transplants: the role of tubular cells in fibrogenesis. *Am J Transplant*. 2005;5(6):1367–1374.
23. Xia JL, Dai C, Michalopoulos GK, Liu Y. Hepatocyte growth factor attenuates liver fibrosis induced by bile duct ligation. *Am J Pathol*. 2006;168(5):1500–1512.